Accepted Manuscript

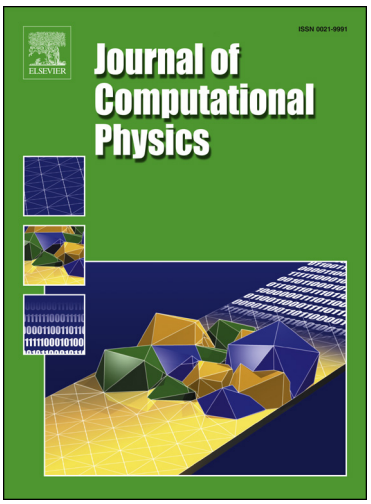

A linear sampling method for through-the-wall radar detection

Matthew Charnley, Aihua Wood

PII: S0021-9991(17)30488-6
DOI: http://dx.doi.org/10.1016/j.jcp.2017.06.035
Reference: YJCPH 7434

To appear in: *Journal of Computational Physics*

Received date: 1 February 2017
Accepted date: 20 June 2017

Please cite this article in press as: M. Charnley, A. Wood, A linear sampling method for through-the-wall radar detection, *J. Comput. Phys.* (2017), http://dx.doi.org/10.1016/j.jcp.2017.06.035

A Linear Sampling Method for Through-the-Wall Radar Detection

Matthew Charnley[1,2] and Aihua Wood[3,4]

Abstract

The through-the-wall inverse scattering problem is analyzed via the linear sampling method. The reciprocity gap formulation of the linear sampling method is used to reconstruct an object within a closed-off room. In order to apply this method, a numerical method to model a point source is needed, along with knowledge of how the numerical fundamental solution differs from the analytic one. Application of the linear sampling method to the Finite Difference Time Domain solution is described and illustrated, and results to reconstruct objects in the through-the-wall setting are shown.

Keywords: FDTD, Through-the-wall imaging, Inverse problems, Linear sampling method, Delta function, Fundamental solution.

1. Introduction

Inverse problems have continually been of mathematical interest for their potential physical applications. One important example of this type of problem is the inverse scattering. Methods for solving the inverse scattering problem have been developed over the last few decades, and are fairly extensive [7]. In particular, the so called 'linear sampling method' has been developed in an attempt to construct a linear problem that can indicate the solution to the very non-linear inverse problem. This method was originally proposed in [6] and expanded upon in [8], [3], and [5], to name a few.

An inverse problem of particular physical interest is that of through-the-wall imaging. In this problem, one wants to use scattered data where both the transmitter and receiver are positioned outside of a solid room to locate and analyze an object inside the room. Previous work has used Doppler-type radar to detect and analyze humans in the through-the-wall setting, whether it be studying human motion with standard Doppler radar [15], noiseforms [14], or micro-Doppler radar, which looks for smaller scale movements such as arm movement [13] and heartbeats [1]. More recent work in this area took place in the master's thesis

[1]Department of Mathematics, Rutgers University, 110 Frelinghuysen Road, Piscataway, NJ 08854, United States. Email: charnley@math.rutgers.edu.
[2]Corresponding Author.
[3]Department of Mathematics and Statistics, Air Force Institute of Technology, Wright-Patterson AFB, OH 45433, United States. Email: Aihua.Wood@afit.edu.
[4]This research was supported by ORISE, and the second author was supported by AFOSR grant F4FGA06071J001.

[12], where a Support Vector Machine was used to detect and analyze the presence of objects in a through-the-wall setting, as well as determine a few properties of the object. The work here seeks to develop a more constructive method for the reconstruction of objects in this particular setting.

In [4] we developed a numerical method for computing the scattered data for a given through-the-wall setup. This work extends [4] by using the same numerical method, but implementing the linear sampling method to perform the reconstructive procedure. The linear sampling method was chosen for this paper because it uses the Helmholtz equation and has been shown to work for related types of problems [9, 10]. As opposed to the previous work, this method does not use a comparison to a wave propagating through an empty room to generate the reconstruction, but has a direct reconstruction method that only uses the data generated by the receivers. Therefore, the reconstruction as stated could be used with only the information gathered in the field, and is much more robust and mathematically sound than the previous method.

An interesting technicality that arises in using the reciprocity gap version of the linear sampling method is that the knowledge of how the system responds to a point source is necessary. In the general case, it would be necessary to compute the Green's function of the background medium. This would involve solving a forward problem and computing the scattered data from a large number of points inside the room, which would be computationally prohibitive to solving this inverse problem. In order to avoid needing to numerically simulate the forward problem at every point that will be tested, it would be ideal to use the fundamental solution of the Helmholtz equation to compute the scattered data from a point source. However, the numerical method does not generate the fundamental solution exactly because of how the waves propagate through the grid and the inability to exactly implement a point source into the FDTD method. Therefore, how the numerical solution differs from the normal fundamental solution needs to be determined so that this modified fundamental solution can be used in the linear sampling method, reducing the need for extra numerical computations as a result of the linear sampling method.

The main development in this paper is the approach to simulating a delta function as the source term in the Finite Difference Time Domain method. As discussed already, in order to use the linear sampling method, the response of the system to a point source is needed, and being able to relate the numerical data being generated to the analytic fundamental solution will allow the method to be carried out without needing to numerically simulate the response to a point source at every point that needs to be tested. This paper then seeks to apply this approach to using the linear sampling method for through-the-wall detection and analysis. While the linear sampling method is not new, the application to through-the-wall imaging, as well as the use of the Finite Difference Time Domain method to generate the data for the linear sampling method, have not been found in the literature to date. The hope is that methods like this one can be applied to physical situations where through-the-wall imaging is desired.

This paper will proceed as follows. Section 2 will outline the version of the linear sampling method that is used in this reconstruction method, the same as the one outlined in [5]. Section 3 describes the method used

to numerically simulate the fundamental solution of the Helmholtz equation, allowing for the calculation of the appropriate fundamental solution to be used in the linear sampling method. Section 4 will show some reconstructions using this method to both validate this particular numerical reconstruction, as well as to extend the calculations to the through-the-wall setting, which does not satisfy all of the assumptions of the normal linear sampling method approach. Section 5 will give a discussion of the results as well as some potential avenues for future work.

2. Linear Sampling Method

The linear sampling method is a procedure developed for solving the inverse scattering problem for the Helmholtz equation [6]. In particular, the method outlined in [5] uses the reciprocity gap approach, which uses a point source as the impulse for the Helmholtz equation instead of a plane wave. This is an important distinction for the problem considered here, as the desired physical system uses a localized source for the reconstruction instead of an ambient plane wave. The general formulation involves an obstacle $D \subset \mathbb{R}^2$ that is embedded in a region $B \subset \mathbb{R}^2$ of the background media where the index of refraction (except for the object D) is constant. As discussed in Section 4, this is one of the main assumptions that is violated when this method is applied to the through-the-wall setting. If $k(x)$ is defined to be the wave number $k^2(x) = k^2 n(x)$, where $n(x)$ is the index of refraction as a function of position, the direct scattering problem is to solve

$$\Delta u + k^2(x)u = 0 \qquad \mathbb{R}^2 \setminus \{x_0\} \tag{1}$$

$$u = u^s + u^i \tag{2}$$

$$\lim_{r\to\infty} \sqrt{r}(\partial_r u^s - iku^s) = 0 \tag{3}$$

where u^i is taken to be the fundamental solution to the Helmholtz equation in the background medium with source at x_0.

To finish setting up the reciprocity gap method, another domain Ω is chosen so that $D \subset \Omega \subset B$ and Ω has smooth boundary Γ, as shown in Figure 1. This Γ will be the curve on which measurements are taken.

If ν is the outward normal to Γ, the *reciprocity gap functional* is defined by

$$\mathcal{R}(u, v) = \int_\Gamma (u\partial_\nu v - v\partial_\nu u)ds$$

where u and v are both solutions to the Helmholtz equation in $\Omega \setminus \bar{D}$. In particular, v is chosen to be a Herglotz wave function with kernel g, *i.e.*

$$v_g(x; z) = \int_{-\pi}^{\pi} e^{ikx\cdot d} g(d; z)\ ds(d)$$

where the parameter z is a point in B, and $g(\cdot; z)$ is a function in $L^2(S^1)$, where S^1 the unit sphere. The reciprocity gap method then seeks to find an approximate solution $g(\cdot; z)$ to the integral equation

$$\mathcal{R}(u, v_g) = \mathcal{R}(u, \Phi_z) \qquad \forall u \in U \tag{4}$$

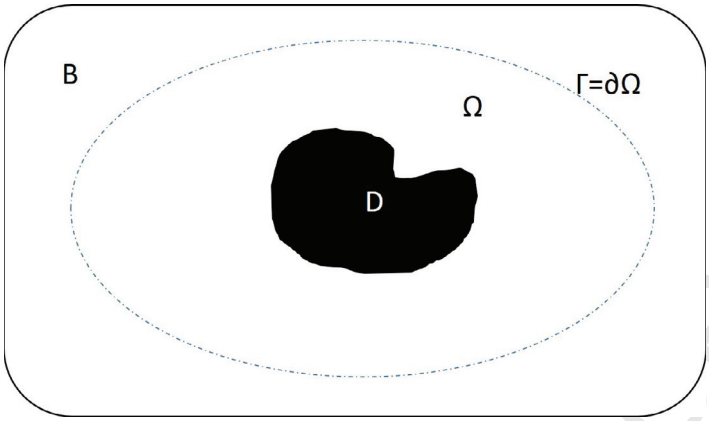

Figure 1: Diagram of the different regions involved in the linear sampling method.

for each z, where Φ_z is the fundamental solution to the background Helmholtz equation with source at z, and U is the set of all solutions to the scattering problem (1)-(3) with x_0 lying in some curve $C \subset B \setminus \Omega$ that is homotopic to Γ. The result that will be used to reconstruct the obstacle D is Theorem 3.1 from [5]:

Theorem 1. *Assume that* $\mathfrak{Im}(n(x)) \geq c > 0$ *for all* $x \in D$.

(a) If $z \in D$, *then there exists a sequence* $\{g_n\} \in L^2(S^1)$ *such that*

$$\lim_{n\to\infty} \mathcal{R}(u, v_{g_n}) = \mathcal{R}(u, \Phi_z)$$

for all $u \in U$. *Furthermore,* v_{g_n} *converges in* $L^2(D)$.

(b) If $z \in \Omega \setminus D$, *then for every sequence* $\{g_n\} \in L^2(S^1)$ *so that*

$$\lim_{n\to\infty} \mathcal{R}(u, v_{g_n}) = \mathcal{R}(u, \Phi_z)$$

for all $u \in U$, *we have that*

$$\lim_{n\to\infty} ||v_{g_n}||_{L^2(D)} = \infty.$$

This gives a method for determining the location of the obstacle D. First, assuming that a region of the room that contains the obstacle is known, and that a set of points are chosen to fill this region. Then, at each of these points z, the solution $g(\cdot; z)$ (or an approximate version) is calculated. By calculating an accurate approximation, it is expected that the norm of this g function will be large if $z \notin D$, and small otherwise. Thus, the norm of this g function can be used to indicate where the obstacle is. This method is implemented in Section 4.

3. Numerical Modeling of a Delta Function

As discussed in Section 2, the execution of the linear sampling method requires the solution u to the Helmholtz equation to be generated by a point source with background fundamental solution Φ. Thus, a

numerical method for generating the fundamental solution to the Helmholtz equation must be developed; that is, a way to simulate the radiation emanating from a point source. It would also be very helpful to know how the solution resulting from this numerical modeling of a point source differs from the analytic fundamental solution to the Helmholtz equation, so that this value can be predicted instead of needing to be recalculated for every instance of the Φ_z defined in Section 2. From the work in [4], however, the generated data is in the form of electric and magnetic fields, and not solutions to the Helmholtz equation. Thus, these results must be prepared properly in order to apply the linear sampling method. This process requires three steps: generating a solution to the Helmholtz equation from the given data, developing a method to model a point source in the FDTD situation, and determining the correction factor needed to match the solution from the numerical method to the analytic fundamental solution.

The first of these steps is not too difficult; since the source has constant frequency ω, it can be assumed that the entire solution also is time-harmonic with frequency ω. In the case of time-harmonic waves, we know that the electric field E satisfies

$$E(x,t) = u(x)e^{i\omega t}$$

for a solution u of the Helmholtz equation with wave number $k = \sqrt{\frac{\omega}{c}}$. Therefore, dividing the electric field by $e^{i\omega t}$ generates a solution of the Helmholtz equation. However, this also assumes that the source is of the form $f(x)e^{i\omega t}$, which, in particular, is complex valued. Since the numerical method can only deal with real-valued functions, this new source needs to be split into its real and imaginary parts, and then recombined at the end. Therefore, generating a solution to

$$\Delta u + k^2 u = f \tag{5}$$

is done via defining two source functions

$$f_R(x,t) = \mathfrak{Re}(f(x)e^{i\omega t}) \qquad f_I(x,t) = \mathfrak{Im}(f(x)e^{i\omega t})$$

computing the electric fields E_R and E_I corresponding to the source functions f_R and f_I respectively, allowing the system to stabilize, and setting

$$u_{num}(x) = e^{-i\omega t}(E_R(x,t) + iE_I(x,t)).$$

This u_{num} is the numerical solution to the Helmholtz equation that will be used for the rest of the paper, which can be computed using the numerical solver once the function f is determined.

For the second step in this process, a numerical solution needs to be determined when $f(x) = \delta_{x_0}(x)$. The main issue dealt with in this section is deriving a method to accurately simulate a Dirac delta function in a numerical scheme. Since the method is a finite difference scheme, the source function needs to be given in the form of fixing the function value at some set of points in the grid. However, the delta function is zero

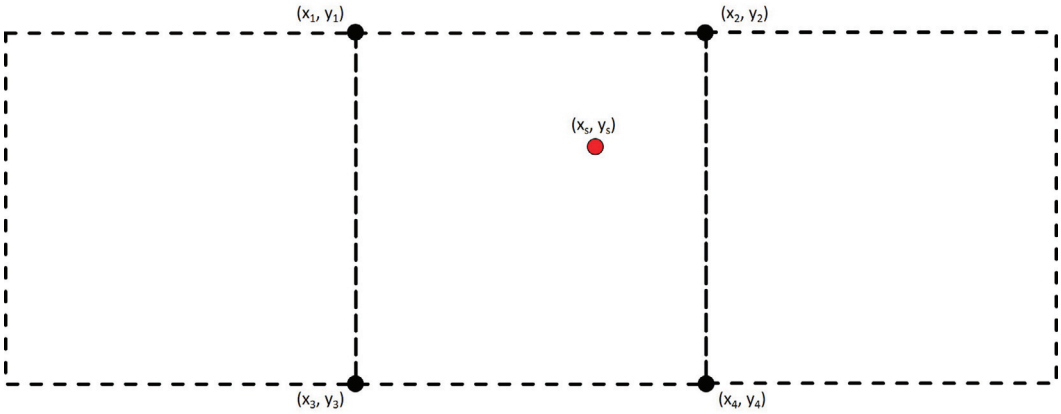

Figure 2: Illustration of the Source Point and the surrounding corners.

everywhere except at the source point, where it takes an infinite value. There could be a few ways to model this on a grid. The first would be to only set the value of a single point in the grid, but make the amplitude of the oscillating source the inverse of the area of the grid squares. This would keep the area under the approximate delta function 1 and leave it centered at a single point. However, as numerical experiments have shown, this does not do a good job of propagating to match the fundamental solution of the Helmholtz equation, because the wave propagation leaves the function much too large at points near the source.

The method developed here will make use of the fact that fundamental solution to the Helmholtz equation in free space is known and the source is located in an area where the background media is constant. In two dimensions, the fundamental solution for the Helmholtz equation

$$\Delta u + k^2 u = \delta_x$$

is

$$\Phi_x(z) = \frac{i}{4} H_0^1(k|x - z|)$$

where H_0^1 is the Hankel function of the first kind of order 0. The numerical method developed and analyzed here to model the point source is by assuming the source is at a defined position that does not fall on any of the grid lines, i.e., the source is strictly contained in one of the squares on the grid. To make the system believe that there is a point source at this location, the values at the four corners of the square containing the source will be fixed to match the fundamental solution. If the source is at (x_s, y_s) as shown in Figure 2 below, then the value of the electric field at corner i, with coordinates (x_i, y_i) is set to be the value

$$f(x_i, y_i) = \frac{i}{4} H_0^1(k\sqrt{(x_s - x_i)^2 + (y_s - y_i)^2}).$$

Using this set up, experimental results show that this choice of source functions give a decent approximation to the amplitude of the standard free-space fundamental solution, as shown in Figure 3. However,

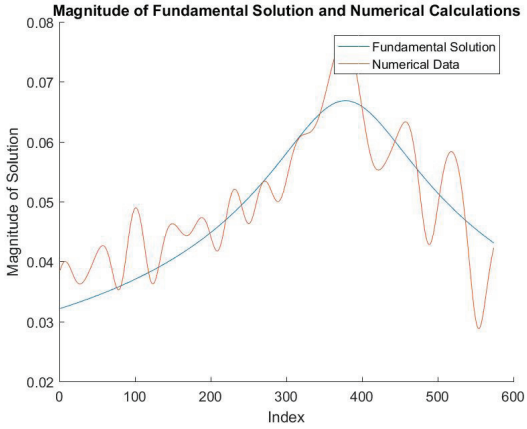

Figure 3: Comparison of the Amplitude of the Fundamental Solution and Numerical Calculation along a Diagonal Line.

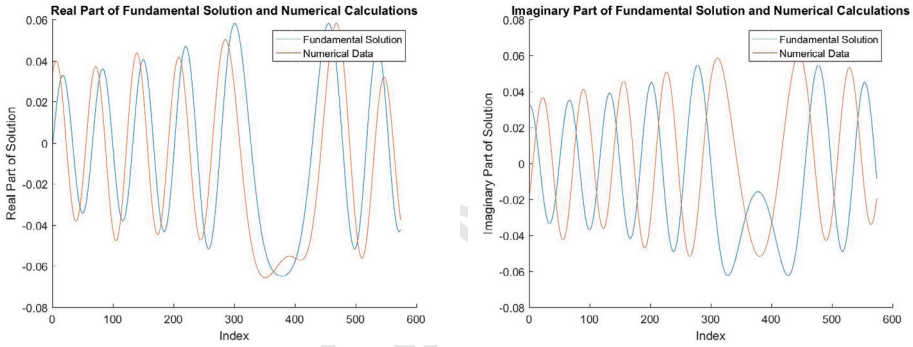

Figure 4: Comparison on the Real and Imaginary Parts of the Numerical Field and the Fundamental Solution.

as illustrated in Figure 4, it is off by a phase factor that varies around the grid. This figure shows the real and imaginary parts of both the numerical and analytic solutions along a diagonal line through the grid. These images suggest that there is the potential to find a phase correction factor that will allow the numerical solution to be predicted from the analytic solution and physical information from the problem. As a first attempt, the phase value of the ratio between the analytic and numeric solution was compared to the distance between the grid point and the source point in a variety of distance metrics. In particular, the ℓ^1, ℓ^2, and ℓ^∞ distances were considered.

Two distinct cases were considered in order to determine if there was a relation here and how it could be utilized. Numerical data was generated with the set of receivers as every grid point on a vertical line, and with the receivers as every grid point on a diagonal line. In looking at the phase discrepancy for each of these two cases, it was seen that the phase discrepancy is linear in the ℓ^2 distance from the source point, as shown in Figure 5. By varying the frequency in the diagonal case, it was also seen that the slope of this

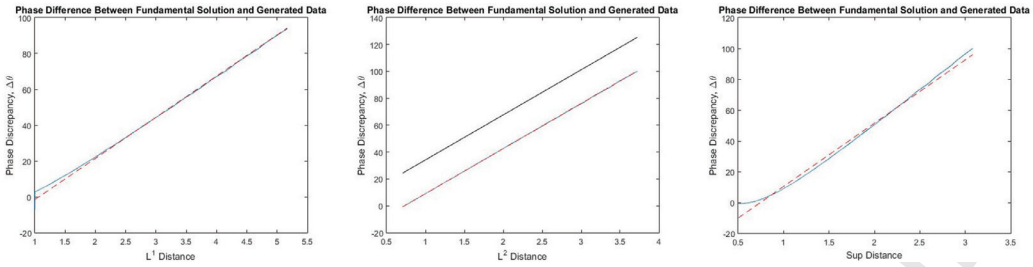

Figure 5: Phase Discrepancy between predicted and numerical data along a diagonal line.

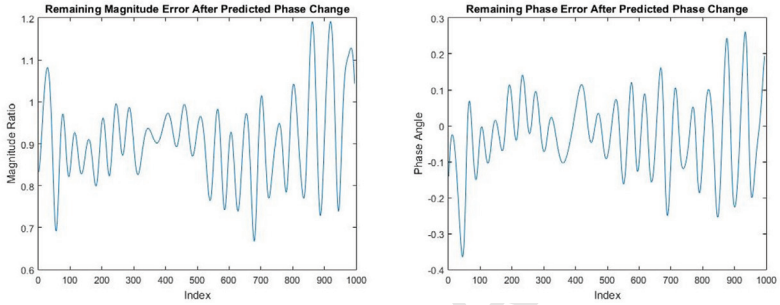

Figure 6: Remaining error in computing the Fundamental Solution after Phase Correction.

phase error depended linearly on frequency, at least within the valid range of frequencies (500 MHz to 1.1 GHz). As a final check of the predicted method, a frequency not used in the previous tests was inputted into the system, and the resulting numerical solution was adjusted by the predicted phase error, and then divided by the analytical solution to the Helmholtz equation. As can be seen in Figure 6, the adjusted numerical solution is fairly close to the analytic solution in both magnitude and phase after adjusting by this correction factor, even over 1000 random points selected on the grid. The slope of the phase discrepancy factor is going to depend on a lot of factors, including the particular way the grid is set up, the CFL constant, and the minimal grid spacing. However, keeping all of these factors constant, it was found that the slope of this predicted line is linear in frequency, allowing for the prediction of the numerical fundamental solution of the Helmholtz equation over a wide range of situations. In Figure 6, the error between the new predicted fundamental solution and the numerical data is displayed. The magnitude and phase errors are shown in the two separate plots, where both of these were computed as ratios; a magnitude error of 1 and a phase error of 0 would mean that the solution has been matched exactly.

In Figure 5, the solid blue line is the phase difference between the predicted and calculated data, and the dashed red line is the best linear fit to this data. In the middle plot, for the ℓ^2 distance, the solid line above the other two is the predicted phase discrepancy slope and intercept fit to the frequency data in the other trials. The black and blue lines do not match, however they are parallel and off by approximately 6π, which

does not affect the result because everything is 2π periodic. Therefore, letting $\eta(d)$ be this phase discrepancy function, the numerical method presented above for a point source centered at (x_0, y_0) generated scattered data (in free space) that can be approximated by

$$\hat{\Phi}_{(x_0,y_0)}(x,y) = \frac{i}{4}H_0^{(1)}(k\sqrt{(x-x_0)^2+(y-y_0)^2})e^{i\cdot\eta(\sqrt{(x-x_0)^2+(y-y_0)^2})} \tag{6}$$

This approximate function will show up in the numerical reconstruction method in the next section.

4. Through-the-Wall Reconstruction

Following [5], computing the function g from the measured scattering data can be written in terms of a compact operator; in particular, finding g amounts to inverting such an operator. Recall from the definitions in Section 2 that Γ is the curve where measurements are being taken and C is a curve outside of Γ that is homotopic to Γ where the source point can be located. By analyzing the form of (4), it can be seen that for each point z it can be written as

$$\mathcal{A}g(\cdot;z) = \phi(\cdot;z) \tag{7}$$

where $\mathcal{A}$ is an integral operator from $L^2(S^1)$ to $L^2(C)$ with integral kernel

$$A(x_0,\hat{d}) = \mathcal{R}(u(\cdot;x_0), v(\cdot;\hat{d}))$$

and $u(x;x_0)$ is the scattered data at x with point source x_0 and

$$v(x,\hat{d}) = e^{ik\hat{d}\cdot x}.$$

The right hand side ϕ is defined by

$$\phi(x_0,z) = \mathcal{R}(u(\cdot;x_0), \hat{\Phi}(\cdot;z))$$

where the normal fundamental solution Φ has been replaced by the numerical approximation $\hat{\Phi}$ developed in the previous section. Since the operator $\mathcal{A}$ is compact, a regularization method is necessary to invert this operator with noisy data. Using Tikhonov regularization as described in [2], the operator will be inverted by solving for an approximate g_α in

$$(\alpha + \mathcal{A}^*\mathcal{A})g_\alpha(\cdot;z) = \mathcal{A}^*\phi(\cdot;z)$$

where α is the regularization parameter. Since the operator $(\alpha + \mathcal{A}^*\mathcal{A})$ is invertible for any $\alpha > 0$, normal methods can be used to invert this matrix. Morozov's discrepancy principle is also used to find the appropriate regularization parameter α. From these calculations, we then compute the indicating function G,

$$G(z) = ||\phi(\cdot,z)||_{L^2(C)}/||g_\alpha(\cdot,z)||_{L^2(S^1)}$$

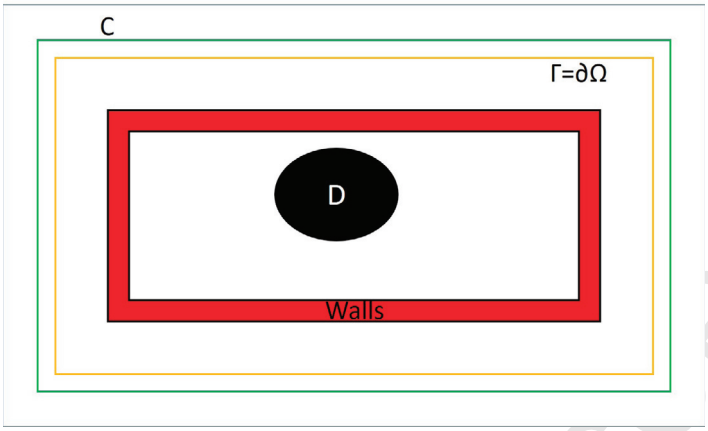

Figure 7: Sketch of the room outlining the surfaces defined in the general Linear Sampling Method.

where, as in our previous work [4], this function can be used to discover where the obstacle D is. Comparing this to Theorem 1 in Section 2, it is seen that for this G function, the value will be large for $z \in D$, and small for $z \notin D$. Therefore, superlevel sets of the G function will be plotted in order to find the location of the object.

In order to generate the scattered data, the curve Γ was taken to be a surface parallel to each of the walls of the room, a fixed distance away from the wall, and data was gathered at each grid point in this range. The possible source points followed a similar path around the outside of the room. Figure 7 outlines all of these surfaces for this given problem setup. Since everything in the calculations done in this work is on a finite difference grid, all of the corresponding integrals are computed via trapezoidal approximations.

There will be three main types of reconstruction, each outlined in their respective sections below.

4.1. Validation of Method

The first set of reconstructions will serve to validate the method that is described above. For this case, the room will be set up without walls and there will just be one object in the center of the area. Previous works like [5] have shown that the linear sampling method works well in cases where the Helmholtz equation is solved directly, so the particular development here that needs to be checked is the use of the FDTD method to generate a solution to the Helmholtz equation.

In looking at the results, there are some stark differences between these and the ones presented in [5] and [11]. Since all of the calculations here were done numerically with a finite difference scheme and data is only known on a grid, the value of the G function can only be evaluated at a discrete set of points. Thus, these results graphs show super-level sets of the G function instead of level curves. Discussion about the actual content of the results will be in Section 5.

Each of the examples below will show the results of computing the G function discussed in the previous

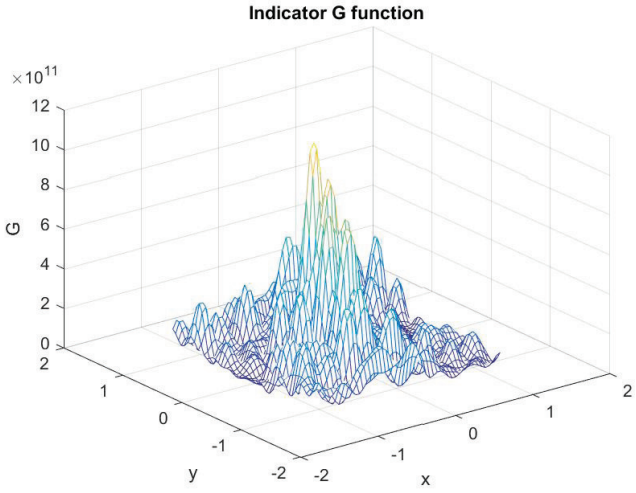

Figure 8: Mesh plot of the G function for Example 1.

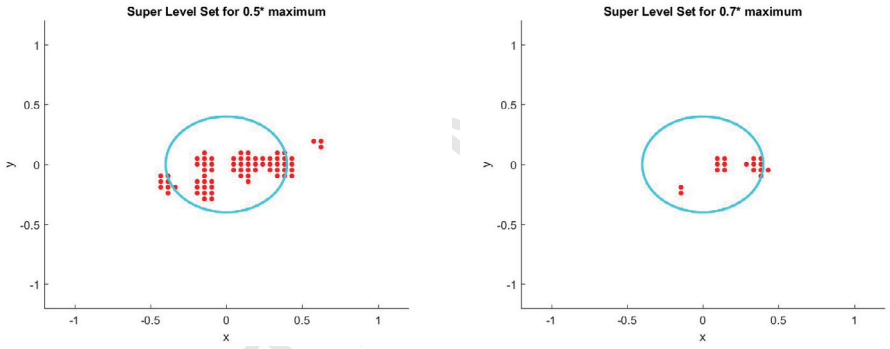

Figure 9: Plots of the superlevel sets of the G function for Example 1.

section. There will be three plots for each example. The first shows a mesh plot of the function G over a square in the middle of the room. The other two plots will show the super level sets of the G function for two different fractions of the maximum value of G on the square. These two plots also include an outline of the object that caused the scattering pattern.

The first example, shown in Figures 8 and 9, includes an object that is centered with regards to where all of the sources and receivers are.

The second example has an off-center object that is smaller. The reconstruction in this case is shown in Figures 10 and 11.

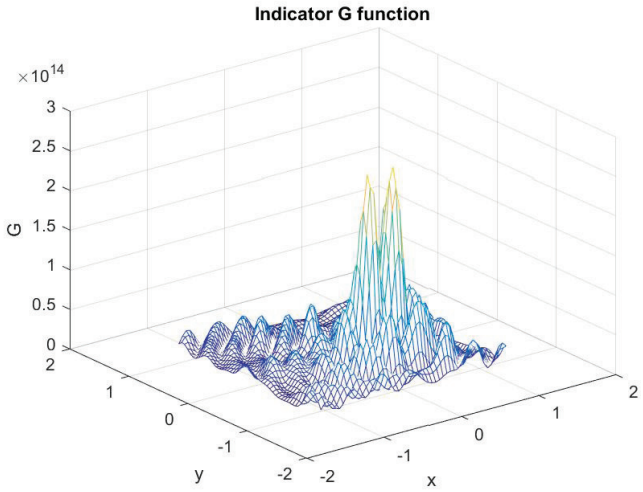

Figure 10: Mesh plot of the G function for Example 2.

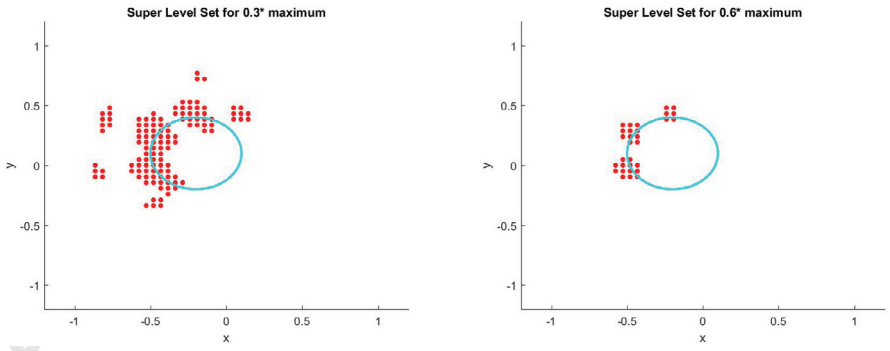

Figure 11: Plots of the superlevel sets of the G function for Example 2.

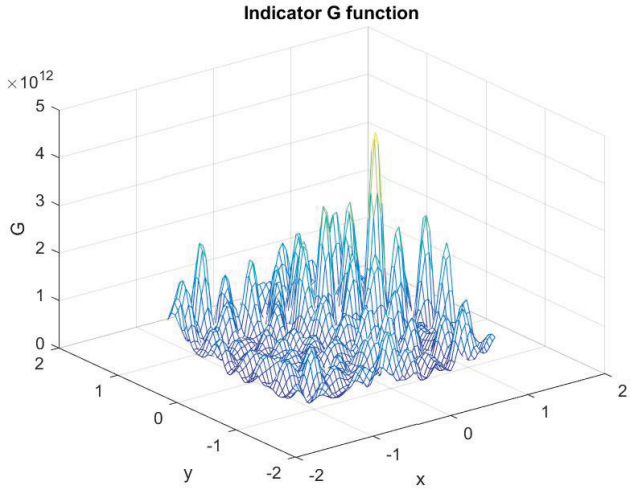

Figure 12: Mesh plot of the G function for Example 3.

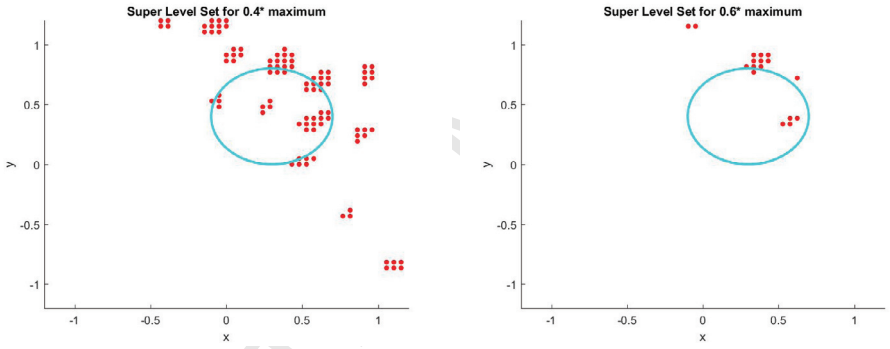

Figure 13: Plots of the superlevel sets of the G function for Example 3.

4.2. Full Data Reconstruction

The next set of reconstructions include the walls of the room. Adding the walls to the room breaks one of the main initial assumptions for the linear sampling method, namely that the region B, in which the curves Γ and C lie, has constant index of refraction outside of the obstacle D. Since the walls have a different index of refraction from free space and measurements need to be taken outside of the walls, it is impossible to meet these requirements to apply the linear sampling method as stated. However, as can be seen in the results below, the numerical method described above is still able to detect the object, although the reconstruction is less accurate than in the simulations without walls. There are two examples in this section, the first of which is shown in Figures 12 and 13, and the second appears in Figures 14 and 15.

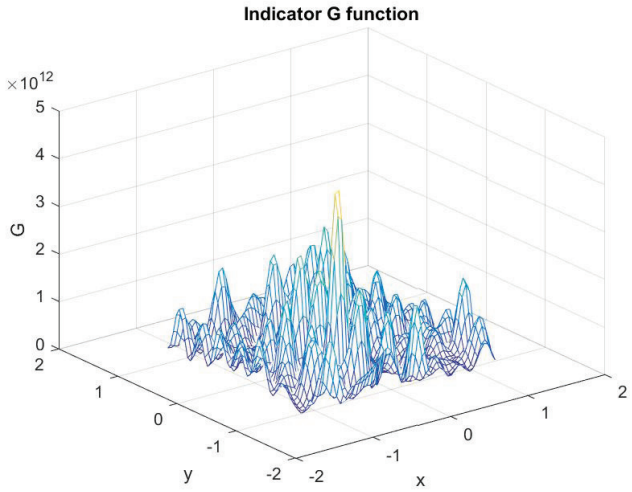

Figure 14: Mesh plot of the G function for Example 4.

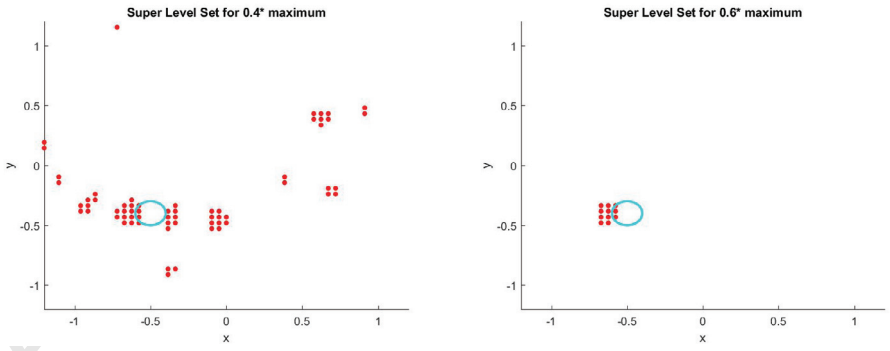

Figure 15: Plots of the superlevel sets of the G function for Example 4.

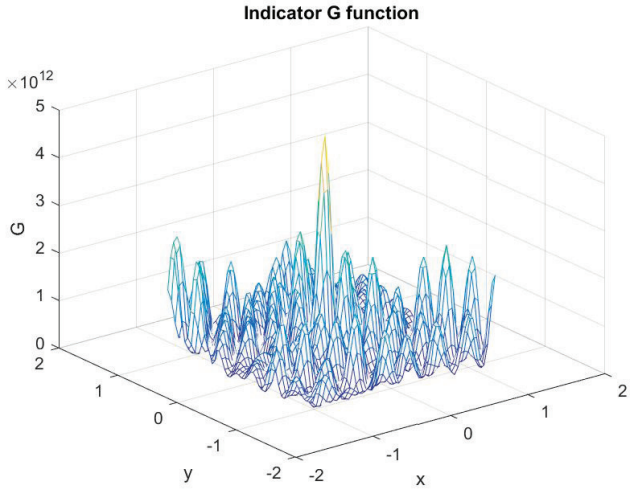

Figure 16: Mesh plot of the G function for Example 5.

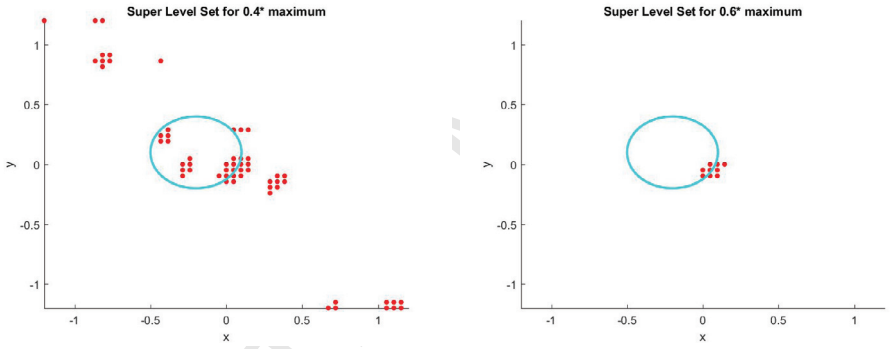

Figure 17: Plots of the superlevel sets of the G function for Example 5.

4.3. Partial Data Reconstruction

The final set of reconstructions are partial aperture reconstructions, assuming that sources can only be placed and measurements can only be taken on one side of the room. This particular situation is more applicable to the given physical problem, because in a physical situation where one wants to locate and analyze an object within a room, it may only be possible to access one external wall of the room. It is expected that these kinds of reconstructions will be much less accurate than the full data constructions, and that is what is seen here. As can be seen in Figure 18 and 19, for any point that the reconstruction thinks is in the object, there is a shadow cast behind it, because without data from the other sides of the room, there is no way to determine where the object ends in that direction. Figures 16 and 17 show the same reconstruction with data from all sides of the room, for comparison.

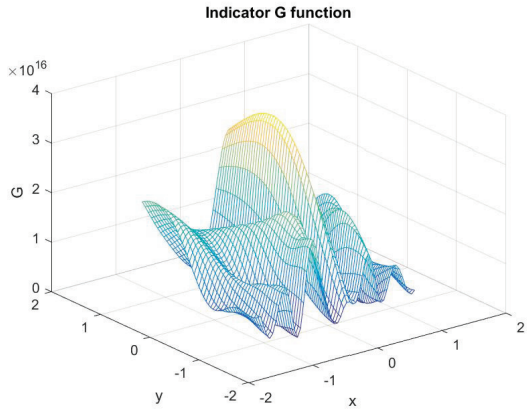

Figure 18: Mesh plot of the G function for Example 5 from partial data.

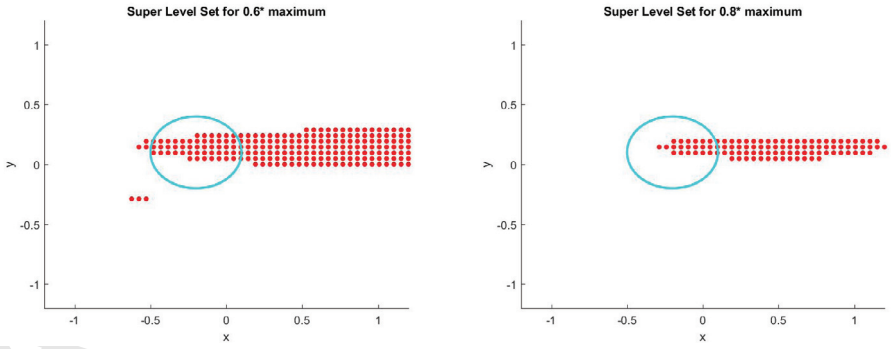

Figure 19: Plots of the superlevel sets of the G function for Example 5 from partial data.

5. Conclusion

The linear sampling method is a fairly well-known method for approximating solutions of inverse scattering problems. However, whether or not FDTD methods could be used to generate data for the linear sampling method, as well as if the method could be applied to the through-the-wall setting, has yet to be explored. The results above show that we have positive results for both of these questions. Section 4.1 shows that, while the reconstructions are not ideal because the indicating function can only be evaluated at a discrete set of points, the method still does a reasonable job of reconstructing the object from the generated field data. If additional *a priori* information was given about the object, like the shape of the object or the number of objects in the domain, a human observer could interpret the data to get a fairly accurate reconstruction. For example, in Figure 9, the G function does not find the entire circular object. However, if it was known in advance that there was a single circular object in the room, it would be very easy to determine the location of the object from this data.

Section 4.2 shows that in the through-the-wall setting the reconstructions get much less accurate, which is to be expected with the addition of walls, but the method can still give an idea of what and where the object is. Finally, Section 4.3 analyzed the partial aperture version of the problem, where data is only known from one side of the room, and showed that the quality of the reconstructions decreased again. As expected, with data from only one side of the room, the method has no way to determine, with any accuracy, where the back edge of the object is.

While this method is significantly more versatile than the previous implementations of the linear sampling method, there are a few limitations to this model. The fact that everything is done with a finite difference solver and the sources are set up within the grid means that everything is done up to a numerical approximation. The numerical errors can cause significant changes because part of the process involves inverting a matrix of these generated values. These generated values also come from a numerically approximated delta function, which, while a good approximation, is still slightly inaccurate. There could also be limitations on resolution, where suitably small objects do not show up entirely correctly, simply because it is hard to distinguish them from slightly larger objects with this near field scattering data.

The added versatility in this algorithm gives it much more flexibility in what the domain can look like and what types of situations it can accommodate. This system can model more complicated geometries than those presented in the previous works, including objects that are nested inside of walls, and multiple objects in any arrangements. It can also handle a smoothly-varying background domain instead of just a uniform constant background, without adding any more numerical complexity. With very little adjustment, this initial set up could be used to handle a large variety of problems in the area of through-the-wall imaging.

All in all, the numerical results give rise to hope for this type of method in the future. The approach of modeling a delta function as a point source for the FDTD method does fairly well in approximating funda-

mental solutions to the Helmholtz equation. This was validated in the case of a free space background, and is assumed to work just as well for non-homogeneous conductivity profiles. The application of this approach to the linear sampling method for object reconstruction showed some potential, but the reconstructions were not as accurate as those where the solution was generated from an integral method as opposed to the Finite Difference Time Domain method. In very complicated domains, the FDTD method may be a quicker way to get a rough estimate of the position and size of an object. From this initial guess, other methods such as non-linear optimization could be applied to approach the actual object.

References

[1] A. S. Bugaev, V. V. Chapursky, S. I. Ivashov, V. V. Razevig, A. P. Sheyko, and I. A. Vasilyev. Through wall sensing of human breathing and heart beating by monochromatic radar. *Proceedings of the Tenth International Conference on Ground Penetrating Radar, 2004.*, 1:291–294, 2004.

[2] F. Cakoni and D. Colton. *A Qualitative Approach to Inverse Scattering Theory*, volume 188 of *Applied Mathematical Sciences*. Springer US, 2014.

[3] F. Cakoni, M. Fares, and H. Haddar. Analysis of two linear sampling methods applied to electromagnetic imaging of buried objects. *Inverse Problems*, 22:845–867, 2006.

[4] M. Charnley and A. Wood. Through-the-wall radar detection analysis via numerical modeling of maxwell's equations. *Journal of Computational Physics*, 313:532–548, 2016.

[5] D. Colton and H. Haddar. An application of the reciprocity gap functional to inverse scattering theory. *Inverse Problems*, 21:383–398, 2005.

[6] D. Colton and A. Kirsch. A simple method for solving inverse scattering problems in the resonance region. *Inverse Problems*, 12:383–393, 1996.

[7] D. Colton and R. Kress. *Inverse Acoustic and Electromagnetic Scattering Theory*, volume 93 of *Applied Mathematical Sciences*. Springer-Verlag New York, 3 edition, 2013.

[8] D. Colton, M. Piana, and R. Potthast. A simple method using morozov's discrepancy principle for solving inverse scattering problems. *Inverse Problems*, 13:1477–1493, 1997.

[9] H. Haddar D. Colton and P. Monk. The linear sampling method for solving the electromagnetic inverse scattering problem. *SIAM Journal of Scientific Computing*, 24:719–731, 2002.

[10] H. Haddar D. Colton and M. Piana. The linear sampling method in inverse electromagnetic scattering theory. *Inverse Problems*, 19:S105–S137, 2003.

[11] H. Haddar and P. Monk. The linear sampling method for solving the electromagnetic inverse medium problem. *Inverse Problems*, 18:891–906, 2002.

[12] Stephanie R. Keith. Discrimination between child and adult forms using radar frequency signature analysis. *Air Force Institute of Technology, AFIT-ENP-13-M-20*, 2013.

[13] R. M. Narayanan, M. C. Shastry, P. H. Chen, , and M. Levi. Through-the-wall detection of stationary human targets using doppler radar. *Progress In Electromagnetics Research B*, 20:147–166, 2010.

[14] Ram M. Narayanan. Through-wall radar imaging using uwb noise waveforms. *Journal of the Franklin Institute*, 345:689–678, 2008.

[15] Shobha Sundar Ram, Yang Li, Adrian Lin, and Hao Ling. Doppler-based detection and tracking of humans in indoor environments. *Journal of the Franklin Institute*, 345:679–699, 2008.